energy&fuels

pubs.acs.org/EF Article

Electrocatalytic Valorization of Organosolv Lignin Utilizing a Nickel-Based Electrocatalyst

Kaili Yan, Yu Zhang, Maobing Tu, and Yujie Sun*

Cite This: *Energy Fuels* 2020, 34, 12703−12709 Read Online

ACCESS | Metrics & More | Article Recommendations | Supporting Information

ABSTRACT: Lignin is a biopolymer that accounts for up to 30% of biomass and is the most abundant aromatic feedstock in nature. Therefore, extraction of valuable aromatic compounds from lignin is regarded as an attractive way for producing various organic chemicals, which are currently derived from fossil fuels. We report an electrochemical approach for the depolymerization of three ethanol organosolv lignins (EOLs), isolated from sweetgum (SW), aspen (AS), and loblolly pine (LP), utilizing a low-cost nickel foam as the working electrode under alkaline conditions. Gas chromatography−mass spectrometry, two-dimensional (2D) heteronuclear single quantum coherence nuclear magnetic resonance (NMR) spectroscopy, and gel permeation chromatography were employed to analyze and quantify the obtained products after electrolysis. Vanillin and syringaldehyde with a combined maximum yield of 17.5% were produced from the electrochemical depolymerization of EOL-SW. Finally, the difference in oxidized products among these three lignin samples was rationalized from the analysis of their native structures.

INTRODUCTION

To meet the ever increasing demand of fuels and chemicals while simultaneously decreasing our reliance on nonrenewable fossil resources, it is imperative to explore the conversion and upgrading of biomass, which is a green carbon source with worldwide abundance.[1−4] As one of the most widely available biomass, lignocellulose is particularly attractive for upgrading to generate value-added products. Over the past few decades, great progress has been achieved in developing biorefinery technologies for the fractionation of lignocellulose to its three primary constituents: cellulose, hemicellulose, and lignin, all of which require further valorization to produce marketable chemicals. Lignin is the second most abundant renewable carbon source after cellulose, and approximately 40−60 million tons of lignin is produced annually, mostly as a byproduct from the paper and pulp industry.[5] Compared to cellulose and hemicellulose, lignin is extremely challenging for depolymerization because of its complex structure and recalcitrant nature. Lignin is an amorphous three-dimensional (3D) biomacromolecule consisting of sinapyl alcohol, conifery alcohol, and *p*-coumary alcohol units, which are cross-linked by C−C and C−O−C bonds forming the recalcitrant backbone of lignin.[6] Currently, the commercial potential of lignin remains largely underexplored (<2% of lignin is recovered for the production of chemical products), and it is almost exclusively burned as a low-grade fuel in the paper and pulp industry, resulting in environmental pollution and resource waste.[7] In contrast, lignin valorization could be very rewarding in that lignin is the largest green carbon source of aromatic building blocks in nature and it represents a sustainable alternative to petroleum-derived BTX (benzene, toluene, and xylene) to obtain aromatic compounds, which play critical roles in many chemical and pharmaceutical processes.[8]

Quite a few chemical conversion strategies have been examined to convert lignin to value-added products, such as steam reforming at high temperature,[9] gasification in supercritical water,[10] pyrolysis,[11] hydrogenation,[12] hydrocracking,[13] hydrothermal fragmentation,[14] and catalytic depolymerization.[15] In general, most chemical conversion approaches necessitate harsh conditions (e.g., high pressure and elevated temperature), and it is difficult to overcome limitations like overoxidation and poor selectivity.[16] The past research efforts have made it clear that cost-effective catalytic systems are critical for successful lignin valorization.

Among many catalytic conversions,[17−19] oxidative depolymerization of lignin enables the production of a great variety of valuable aromatics,[20−23] especially the benzaldehyde derivatives like vanillin and syringaldehyde, which can find applications in the fields of flavor, fragrance, and pharmaceuticals.[24,25] A large number of chemical oxidants, starting from nitrobenzenes[26] to hydrogen peroxide,[27] metal alloy,[28] $LaMnO_3$,[29] Pd/Al_2O_3,[30] $LaFe_{1-x}Cu_xO_3$,[31] and even air,[32,33] have been utilized for the oxidative depolymerization of lignin. Besides, ozonation is another oxidative process for lignin degradation, which is usually conducted at low temperatures (20−40 °C) due to its high reactivity toward all unsaturated structures.[34] Aulin-Erdtman et al. demonstrated that the extensive ozonation of lignin degraded the aromatic moieties while the side chains of the dominant structure could be recovered in the forms of erythronic and threonic acids.

Received: July 9, 2020
Revised: September 3, 2020
Published: September 9, 2020

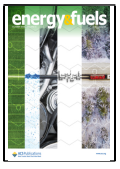

https://dx.doi.org/10.1021/acs.energyfuels.0c02284
Energy Fuels 2020, 34, 12703−12709

Therefore, compared to the other oxidative process, the ozonation process would provide more reliable information on various side chain structures in lignin.[35] Nevertheless, the requirement of stoichiometric amount of chemical oxidants renders these processes less economically attractive for large-scale applications. In contrast, electrocatalytic depolymerization appears very appealing in lignin valorization because of the following reasons: (i) facile control over oxidation via electrochemical parameters (e.g., potential, current, electrolyte, etc.), (ii) electricity-driven oxidation with no chemical oxidants needed, and (iii) operation under ambient conditions.

Since electrocatalytic oxidation has been regarded as an environmentally friendly and sustainable process for lignin degradation,[36] great efforts have been devoted to exploring various electrocatalytic systems for effective conversion of lignin to valuable products. Most studies have centered on noble metal- (e.g., RuO_2 and IrO_2)[37] or toxic metal-based (e.g., Pb/PbO_2)[38,39] electrocatalysts. More recently, redox mediators, like 2,2,6,6-tetramethyl-1-piperidine *N*-oxyl (TEMPO) and 4-acet-amido-TEMPO as catalytic mediators, have also been utilized for the electrocatalytic oxidation of lignin model compounds and natural lignin.[40] Given the increasing motivation in green chemistry, more economically attractive and environmentally friendly electrocatalysts are desired for lignin depolymerization.[41]

Herein, we report a facile electrocatalytic approach for the depolymerization of three native ethanol organosolv lignin (EOL) samples utilizing nickel foam as a low-cost electrocatalyst under alkaline conditions. As a greener alternative to precious or toxic metals, nickel electrodes are known for their stability and catalytic activity for lignin degradation. Under alkaline conditions, NiOOH is formed on the surface of nickel foam that could further increase its catalytic activity and avoid overoxidation of the monomers.[42]

EOLs from three woody biomass, including sweetgum (SW), aspen (AS), and loblolly pine (LP), were directly subjected to electrochemical oxidation on nickel foam in 1.0 M KOH. Post-electrolysis analysis employing gas chromatography−mass spectrometry (GC−MS), two-dimensional (2D) heteronuclear single quantum coherence (HSQC) nuclear magnetic resonance (NMR), and gel permeation chromatography (GPC) was performed to identify and quantify obtained products. Our results demonstrate the effectiveness of nickel in electrochemical depolymerization of lignin with vanillin and syringaldehyde as the primary products from EOL-SW and EOL-AS, whereas no syringaldehyde was detected from the electrolysis of EOL-LP, which was rationalized from the structural analysis of each native lignin sample.

EXPERIMENTAL SECTION

Wood chips ($L \times W \times H$: 1.0 × 1.0 × 0.3 cm^3) including sweetgum (*Liquidambar styraciflua*), loblolly pine (*Pinus taeda*), and aspen were gathered by the Forest Products Laboratory at Auburn University. Nickel foam with purity >99.99% was purchased from MTI. All chemicals and solvents were commercially available and used without further treatment.

Ethanol organosolv lignin (EOL) was precipitated from ethanol organosolv pretreated hydrolysate of each woody biomass.[43] Prior to the pretreatment, wood chips (80 g of dry weight) were soaked in 0.56 L of 65% ethanol solution with 1.0% (w/w) sulfuric acid overnight to achieve sufficient impregnation. The pretreatment was performed at 160 °C (sweetgum and aspen) or 170 °C (loblolly pine) for 1 h in a 2 L Parr batch reactor. Afterward, the reaction was immediately quenched to room temperature in a cold water bath. The liquid hydrolysate fraction was collected via vacuum filtration. EOLs were precipitated by adding threefold DI water into the hydrolysate and collected by vacuum filtration with Whatman No. 1 filter paper. The collected EOLs were washed with threefold warm water to remove the potential contaminations and air-dried for further experiments.

The electro-oxidation of EOL was conducted at room temperature using a BioLogic potentiostat. All of the electrochemical experiments were performed in 1.0 M KOH with a three-electrode configuration, in which a commercially purchased nickel foam was directly used as the working electrode, a Hg/HgO electrode as the reference electrode, and a Pt wire as the counter electrode. Cyclic voltammetry was first scanned from open circuit potential to 0.7 V vs Hg/HgO at 20 mV/s without the lignin sample several times until stable cyclic voltammetry curves were obtained. After the addition of lignin sample (20 mg), cyclic voltammetry was conducted followed by long-term electrolysis at a constant potential.

After electrolysis, the electrolyte was first acidified to pH = 3−4 with 0.5 M H_2SO_4. Afterward, chloroform of the same volume was added to the electrolyte to form a two-phase mixture. The upper layer was the aqueous phase, and the bottom layer was the organic phase. The extraction process was repeated three times, and all of the collected chloroform phase solutions were combined and evaporated at room temperature on a rotary evaporator. The aqueous phase was concentrated at 35 °C on a rotary evaporator as well, and yellow solid products were obtained, which were washed with water several times to remove inorganic salts and finally dried under vacuum conditions.

The chloroform extractive was redissolved in 700 μL of chloroform and analyzed via gas chromatography−mass spectrometry (GC−MS). The GC−MS was equipped with an Agilent 19091S-433 column (30 m × 0.25 mm × 0.25 mm). The injection volume of sample solution was 1 μL with helium as a carrier gas at a flow rate of 1.1971 mL/min. The temperature program was set at 50 °C for 5 min and then increased to 250 °C with a rate of 15 °C per min followed by maintaining the same temperature for another 5 min. The identification of detected compounds from GC−MS results was based on the NIST database. Quantification of target products was performed from the integration of the peak area in the total ion chromatogram (TIC) of each target compound based on the pre-established calibration curves of commercial samples. The yields (%) of vanillin and syringaldehyde were calculated based on the following equation

$$\text{yield (\%)} = \frac{\text{mass of vanillin and syringaldehyde}}{\text{mass of initial EOL sample}} \times 100\%$$

Analysis of native and oxidized EOLs was performed using 2D heteronuclear single quantum coherence (HSQC) NMR. EOLs were dissolved in 500 μL of dimethyl sulfoxide (DMSO)-d_6 and analyzed on a Bruker AVANCE 600 MHZ NMR spectrometer. The spectra were recorded with the Bruker pulse program "hsqcetgpsi", and the parameters used were as follows: the number of collected complex points was 1 K for the ^1H dimension with a delay time of 2 s. The number of scans were 64, and 256 time increments were recorded in the ^{13}C dimension. The Q-HSQC spectra were collected using the following parameters: the ^1H dimension (F2) was acquired from 11.28 to −1.88 ppm with 2048 data points, and the ^{13}C dimension (F1) was acquired from 185 to −35 ppm with 256 increments. The number of scans was 16, and the recycle delay was 10 s. Acquisition times of 0.19 and 0.0058 s were used for ^1H and ^{13}C, respectively. The total acquisition time was 11 h 40 min. Afterward, Fourier transformation and phase correction were applied in both dimensions on spectra with MNova X64. The molecular weights of the native and oxidized EOLs were determined via gel permeation chromatography (GPC) using an ultraviolet (UV) detector. The column was equipped with a PL-gel 10 mm mixed-B 7.5 mm id column, which was calibrated with PL polystyrene standards. The calibration curve of GPC is shown in Figure S1. The lignin samples were dissolved in tetrahydrofuran followed by sonication for at least 1 h prior to filtering through a PFTE membrane (0.2 μm).

https://dx.doi.org/10.1021/acs.energyfuels.0c02284
Energy Fuels 2020, 34, 12703−12709

RESULTS AND DISCUSSION

Prior to electrocatalytic depolymerization, all of the lignin samples derived from wood chips, including sweetgum, aspen, and loblolly pine (EOL-SW, EOL-AS, and EOL-LP), were isolated via an organic solvent extraction method (see the Experimental Section for details). Such a pretreatment yielded EOLs with high purity and a nativelike lignin structure. Subsequent electrochemical studies were conducted in a three-electrode configuration with 1.0 M KOH as the electrolyte. With the aim of low-cost and green operation in mind, a commercially available nickel foam (NF) was directly utilized as the working electrode. As shown in Figure 1, NF exhibited

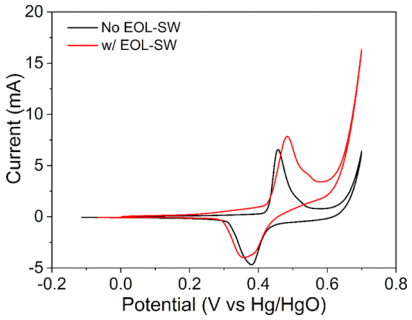

Figure 1. Cyclic voltammograms of nickel foam in 1.0 M KOH before and after the addition of 20 mg of EOL-SW (scan rate: 20 mV/s).

the anticipated $Ni^{III/II}$ redox couple in the potential region of 0.3−0.5 V vs Hg/HgO,[44] followed by an anodic current rise after 0.6 V vs Hg/HgO, which could be attributed to the O_2 evolution reaction (OER). Upon the addition of 20 mg of the EOL-SW sample, an apparent anodic current increase around the $Ni^{III/II}$ redox couple could be observed, indicating the oxidation of the lignin substrate on NF. To delineate the oxidation products, controlled potential electrolysis was first conducted for EOL-SW at three applied potentials, 0.4, 0.5, and 0.6 V vs Hg/HgO for 1 h. The post-electrolysis electrolytes were neutralized and then exacted via chloroform (see the Experimental Section for details). The resultant oxidation products in both organic and aqueous layers were collected and analyzed individually.

The oxidation products of EOL-SW in the organic phase were characterized via GC−MS. As shown in Figure S2, a range of oxidation products could be detected in the retention time between 5 and 25 min. Vanillin and syringaldehyde were detected as the major products with retention times of 11.3 and 13.5 min, respectively. The identity of vanillin and syringaldehyde was confirmed by comparing their corresponding retention time and mass spectrum with those of commercial standard samples (Figures S3 and S4). Based on the calibration curves (Figure S5) derived from the purchased model compounds, the yields of vanillin and syringaldehyde obtained at three different electrolysis potentials could be quantified. Table 1 compares the yields resulting from different electrolysis experiments. For 1 h electrolysis, the combined yield of vanillin and syringaldehyde was 11.0% when the applied potential was 0.4 V vs Hg/HgO, implying that oxidative lignin depolymerization takes place even before reaching the anodic peak potential of NF. If the applied potential was 0.5 V vs Hg/HgO, an increased yield of 17.5% was obtained, consistent with the high anodic current observed around 0.5 V vs Hg/HgO (Figure 1). However, further anodic

Table 1. Combined Yields of Vanillin and Syringaldehyde Obtained from the Electrocatalytic Depolymerization of EOL-SW on Nickel Foam under Different Conditions

entry	potential (V vs Hg/HgO)	electrolysis time (h)	yield (%)
1	0.4	1	11.0
2	0.5	1	17.5
3	0.6	1	9.5
4	0.5	0.5	10.5
5	0.5	2	12.5

shifting of the applied potential to 0.6 V vs Hg/HgO resulted in a decrease of the combined yield of vanillin and syringaldehyde to 9.5%, most likely due to the involvement of OER, which is the primary competing reaction at high anodic potentials. Hence, it was apparent that 0.5 V vs Hg/HgO was the optimal applied potential for the depolymerization of EOL-SW on NF in 1.0 M KOH. To assess the impact of electrolysis time, we further varied the duration of electrocatalytic oxidation at 0.5 V vs Hg/HgO from 0.5 to 2 h (Figure S6). As included in Table 1, 0.5 h electrolysis led to a combined yield of 10.5% while 2 h resulted in 12.5%, both of which were lower than the 17.5% yield obtained after 1 h electrolysis. The lower yield for the 2 h electrolysis could be due to the overoxidation of vanillin and syringaldehyde during prolonged oxidative electrolysis. Overall, the maximum yield (17.5%) of vanillin and syringaldehyde from EOL-SW was achieved on NF at an applied potential of 0.5 V vs Hg/HgO for 1 h electrolysis in 1.0 M KOH. Notably, the yield of vanillin is higher than previous reported yields obtained via electrolysis,[45,46] which enabled 1.7 and 7 wt % yields of vanillin, respectively.

In addition to the identification and quantification of low-molecular-weight organic products in the chloroform extractives, we also sought to investigate the resultant oxidation products in the aqueous phase, which were expected to have higher molecular weight and larger polarity compared to those in the organic phase. Two-dimensional heteronuclear single quantum coherence spectroscopy (HSQC) NMR and gel permeation chromatography (GPC) were performed to probe the structural and molecular weight changes of post-electrolysis products in the aqueous phase, respectively. It should be noted that the assignments of 2D HSQC NMR spectra were determined based on the reported results[31] and are compiled in Table S1. The 2D HSQC NMR spectra of EOL-SW prior to and postelectrocatalytic oxidation in the aliphatic region are shown in Figure 2a, and the corresponding substructures are presented in Figure 2b. It is apparent that after electrolysis the NMR signals from the β-O-4 (A) and α-OEt β-O-4′ (A′) substructures were both substantially decreased. In addition, the β−β resinol (B) and phenylcoumaran (C) substructures almost disappeared in the post-electrolysis sample. Furthermore, the 2D HSQC NMR spectra in the aromatic region are also compared in Figure 2c, and the related syringyl (S and S′) and guaiacyl (G) structural units are included in Figure 2d. The much weaker NMR signals of S and S' substructures, together with the nearly disappeared signal of the G unit, after electrolysis, all supported lignin depolymerization during electrolysis. Taken together, our 2D HSQC NMR measurements confirmed the effectiveness of electrocatalytic depolymerization of lignin into useful aromatic compounds.

The molecular weights of the native EOL-SW and the oxidation products in the aqueous phase were also determined

https://dx.doi.org/10.1021/acs.energyfuels.0c02284
Energy Fuels 2020, 34, 12703−12709

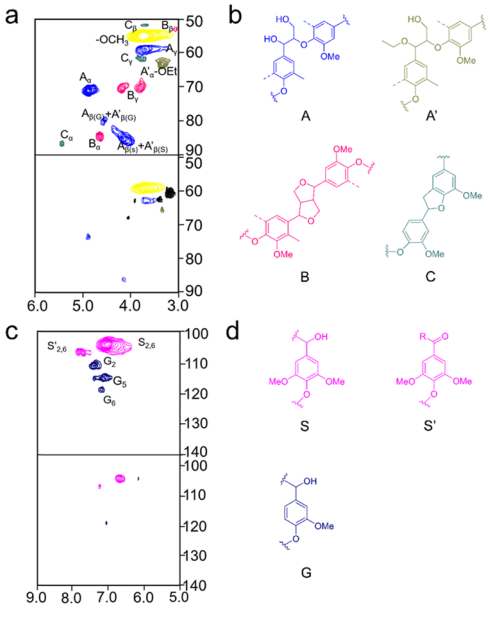

Figure 2. (a, c) HSQC spectra of EOL-SW before (top) and after (bottom) electrochemical oxidation in the aliphatic (a) and aromatic (c) regions. (b, d) Structural units existing in native lignin, including β-O-4 (A), α-OEt β-O-4′ (A′), β-β resinol (B), phenylcoumaran (C), syringyl (S and S′), and guaiacyl (G) units.

via the GPC analysis. The GPC chromatograms are compared in Figure S7. The number-averaged (M_n) and weight-averaged (M_w) molecular weights of the native EOL-SW were 3123 and 5163 g/mol, respectively. Post-electrolysis, the M_n and M_w values of the oxidized lignin sample in the aqueous phase decreased to 2650 and 4435 g/mol, respectively, lower than those of the pristine sample. These GPC results further confirmed the depolymerization of EOL-SW during electrocatalytic oxidation on NF.

The success of electrocatalytic oxidation in the depolymerization of EOL-SW prompted us to explore the versatility toward other lignin substrates. Therefore, EOL-AS and EOL-LP, which were obtained from an analogous pretreatment, were also utilized for electrochemical depolymerization. As shown in Figure 3, the addition of EOL-AS (Figure 3a) and EOL-LP (Figure 3b) resulted in apparent anodic current rise around the $Ni^{III/II}$ redox feature of NF in 1.0 M KOH, suggesting the oxidation of these lignin samples on NF, similar to the situation observed for EOL-SW (Figure 1). Following the same conditions for the oxidative electrolysis of EOL-SW, 0.5 V vs Hg/HgO for 1 h, controlled potential electrolysis was performed for the EOL-AS and EOL-LP samples. The same post-electrolysis extraction of the electrolyte solutions using chloroform resulted in two phases. The organic phase solutions were analyzed via GC−MS. As shown in Figure S8, both vanillin and syringaldehyde were detected as the primary oxidation products from the electrochemical depolymerization of EOL-AS, showing a combined yield of 11.5%. Even though vanillin could still be identified in the oxidation products of the EOL-LP electrolysis with a yield of 13.0%, interestingly no syringaldehyde trace could be detected in its GC−MS spectrum.

To fully evaluate the impact of the electro-depolymerization method, 2D HSQC has also been conducted to characterize the structure characteristics in the organic phase. As shown in Figure S9, there are well-distinguished signals of A, A′, and B units in the aliphatic region of the organic phase from EOL-SW. In the cases of EOL-AS and EOL-LP, various identifiable peaks could also be observed in the aliphatic region. In addition, many 2D HSQC features could be in the aromatic region for all of the three samples as well, which further support the effectiveness of our electro-depolymerization approach.

Besides the organic phase, products formed in the aqueous phase were also analyzed via GPC. The GPC chromatograms and weight distribution of the native EOL-AS and EOL-LP and their products in the aqueous phase after electrolysis are shown in Figures S10 and 11. As shown in Table 2, the number-averaged molecular weights (M_n) of EOL-AS and EOL-LP samples decreased from 2865 and 2968 to 2664 and 2315 g/mol, respectively. In addition, a more substantial decrease was observed in their weight-averaged molecular weights (M_w), changing from 5338 and 5878 to 3338 and 2770 g/mol, respectively. These results collectively demonstrate the competence of our nickel foam in the electrochemical depolymerization of lignin samples, including not only EOL-SW but also EOL-AS and EOL-LP. The key steps of electrochemical depolymerization are proposed in Figure 4, wherein a secondary benzylic alcohol group at the C_α is first oxidized followed by the cleavage of the β-O-4 linkage, which affords low molecular compounds. Specifically, in the electro-oxidation step, a secondary benzylic alcohol group at the C_α position is oxidized to ketone by NiOOH. Subsequently, the β-carbon is dehydrogenated followed by C−O bond cleavage.

To elucidate the correlation between the native lignin structure and the oxidation products after electrolysis, 2D HSQC spectra of the aforementioned three lignin samples are compared in Figure 5. Specifically, the 2D HSQC spectra of

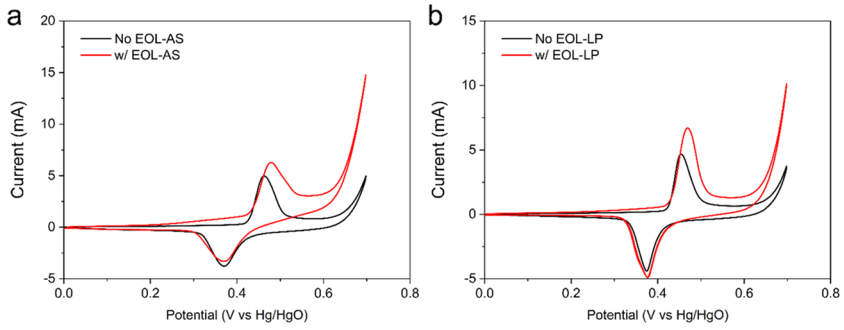

Figure 3. Cyclic voltammograms of nickel foam in 1.0 M KOH before and after the addition of 20 mg of EOL-AS (a) and EOL-LP (b) (scan rate: 20 mV/s).

https://dx.doi.org/10.1021/acs.energyfuels.0c02284
Energy Fuels 2020, 34, 12703−12709

Table 2. Number-Average (M_n) and Weight-Average (M_w) Molecular Weights of Three Organosolv Lignin Samples before and after Electrolysis

	EOL-SW		EOL-AS		EOL-LP	
lignin molecular weight	M_n (g/mol)	M_w (g/mol)	M_n (g/mol)	M_w (g/mol)	M_n (g/mol)	M_w (g/mol)
before electrolysis	3123	5163	2865	5338	2968	5878
after electrolysis	2650	4435	2664	3338	2315	2770

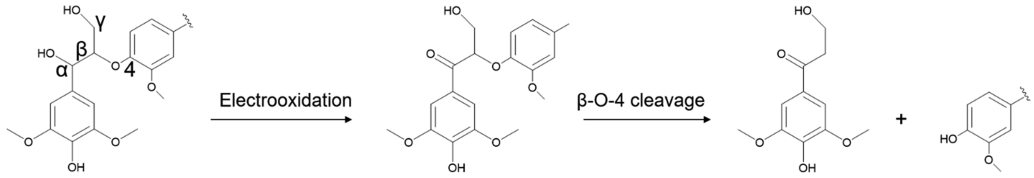

Figure 4. Schematic representation of the oxidation and cleavage of the lignin β-O-4 unit.

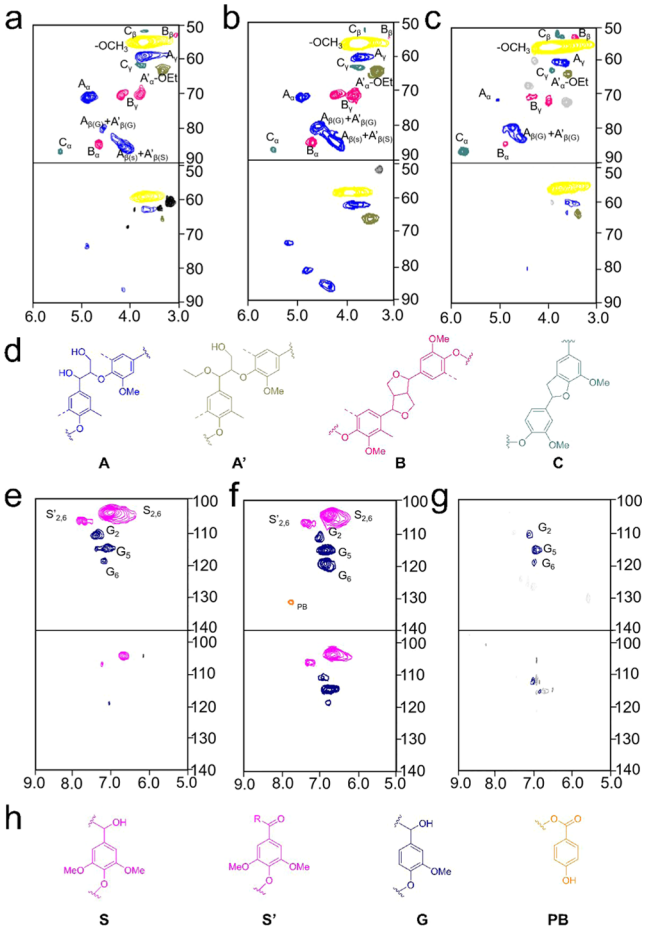

Figure 5. 2D HSQC spectra of EOL-SW (a), EOL-AS (b), and EOL-LP (c) samples before (top) and after (bottom) electrolysis in the aliphatic region together with corresponding structures (d). 2D HSQC spectra of EOL-SW (e), EOL-AS (f), and EOL-LP (g) samples before (top) and after (bottom) electrolysis in the aromatic region together with corresponding structures (h).

EOL-SW, EOL-AS, and EOL-LP samples in the aliphatic region prior to and post-electrolysis are presented in Figure 5a–c, respectively. The possible units, A, A′, B, and C, of the corresponding substructures containing aliphatic carbons are shown in Figure 5d. It is clear to see that all of the three lignin samples possess these four substructural units in their pristine state. After electrolysis, all of the corresponding signals in the aliphatic region substantially decreased, in agreement with the depolymerization of these lignin samples during electrocatalytic oxidation. In contrast, very different structural features of these three lignin samples could be observed in the aromatic region. Both EOL-SW (Figure 4e) and EOL-AS (Figure 5f) contain the syringyl (S and S′) and guaiacyl units (G). In striking contrast, no syringyl units could be observed in the 2D HSQC spectrum of the EOL-LP (Figure 5g). As shown in Figure 5h, the syringyl units (S and S′) feature methoxy groups at the 3′ and 5′ positions of a benzyl ring, while the guaiacyl unit (G) only has one methoxy group at 3′. After electrocatalytic depolymerization, S and S′ units will lead to the formation of syringaldehyde and the guaiacyl units will result in the production of vanillin. The absence of syringyl units in loblolly pine lignin dictates that there should be no syringaldehyde detected after depolymerization, which is consistent with our experimental results. On the other hand, because of the existence of guaiacyl units (G) in all of the three lignin samples, their common oxidation product is vanillin. According to the previous literature,[47] softwood lignins are mainly composed of G units, together with small proportions of H units and a trace amount of S units. In contrast, hardwood lignin generally results from G and S units and small quantities of H units. In our case, loblolly pine is a softwood, while both sweetgum and aspen are hardwood. Therefore, our experimental results are also consistent with previous reports.

To provide the quantitative analysis of the aqueous phase, Q-HSQC spectra were collected using the pulse program described in an earlier study.[48] The integration values of the lignin structure were estimated from Figure S13, and the results are summarized in Table S2. As shown in Table S2, the amounts of main substructures in these three organosolv lignin samples decreased substantially after electrolysis. This result demonstrates that significant cleavage of organosolv lignin structures occurs under electro-oxidation conditions.

CONCLUSIONS

A facile and effective electrochemical approach was presented for the depolymerization of three native lignin samples isolated from ethanol organosolv pretreatment of different biomass, including sweetgum, aspen, and loblolly pine. Our results demonstrate that low-cost and commercially available nickel foam could be directly employed as a competent working electrode for the oxidative depolymerization of lignin samples. Vanillin and syringaldehyde were determined as the primary small molecule products from the electrochemical depolyme-

https://dx.doi.org/10.1021/acs.energyfuels.0c02284
Energy Fuels 2020, 34, 12703−12709

rization of sweetgum and aspen organosolv lignin with the maximum yield of 17.5% achieved for the sweetgum electrolysis. Detailed structure analysis of these lignin samples was also conducted to elucidate the structure−product correlation and rationalize the absence of syringaldehyde in the post-electrolysis products of loblolly pine organosolv lignin. To further improve the performance of NF catalysts, 3D hierarchically porous nickel-based electrocatalyst (hp-Ni) could be prepared by electrodeposition of metallic Ni nanoparticles on nickel foam.[49]

■ ASSOCIATED CONTENT

Supporting Information

The Supporting Information is available free of charge at https://pubs.acs.org/doi/10.1021/acs.energyfuels.0c02284.

Additional experimental data and GC−MS, Q-HSQC NMR, and GPC results (PDF)

■ AUTHOR INFORMATION

Corresponding Author

Yujie Sun − *Department of Chemistry, University of Cincinnati, Cincinnati, Ohio 45221, United States;* orcid.org/0000-0002-4122-6255; Email: yujie.sun@uc.edu

Authors

Kaili Yan − *Department of Chemistry, University of Cincinnati, Cincinnati, Ohio 45221, United States*

Yu Zhang − *Department of Chemical and Environmental Engineering, University of Cincinnati, Cincinnati, Ohio 45221, United States*

Maobing Tu − *Department of Chemical and Environmental Engineering, University of Cincinnati, Cincinnati, Ohio 45221, United States*

Complete contact information is available at: https://pubs.acs.org/10.1021/acs.energyfuels.0c02284

Notes

The authors declare no competing financial interest.

■ ACKNOWLEDGMENTS

Y.S. acknowledges financial support of the Herman Frasch Foundation (820-HF17), the National Science Foundation (CHE-1914546), and the University of Cincinnati. M.T. thanks the University of Cincinnati, Office of the Vice President for Research—Collaborative Research Advancement Grants-Pilot Program, and URC Graduate Student Stipend and Research Cost Program. NMR experiments were performed on a Bruker AVANCE NEO 400 MHz NMR spectrometer (funded by NSF-MRI Grant CHE-1726092).

■ REFERENCES

(1) Huber, G. W.; Iborra, S.; Corma, A. Synthesis of transportation fuels from biomass: chemistry, catalysts, and engineering. *Chem. Rev.* **2006**, *106*, 4044−4098.

(2) Chakar, F. S.; Ragauskas, A. J. Review of current and futures softwood kraft lignin process chemistry. *Ind. Crops Prod.* **2004**, *20*, 131−141.

(3) Bozell, J. J.; Petersen, G. R. Technology development for the production of biobased products from biorefinery carbohydrates—the US Department of Energy's "Top 10" revisited. *Green Chem.* **2010**, *12*, 539−554.

(4) Thakur, V. K.; Thakur, M. K.; Raghavan, P.; Kessler, M. R. Progress in green polymer composites from lignin for multifunctional applications: a review. *ACS Sustainable Chem. Eng.* **2014**, *2*, 1072−1092.

(5) Ververis, C.; Georghiou, K.; Christodoulakis, N.; Santas, P.; Santas, R. Fiber dimensions, lignin and cellulose content of various plant materials and their suitability for paper production. *Ind. Crops Prod.* **2004**, *19*, 245−254.

(6) Pan, X.; Kadla, J. F.; Ehara, K.; Gilkes, N.; Saddler, J. N. Organosolv ethanol lignin from hybrid poplar as a radical scavenger: relationship between lignin structure, extraction conditions, and antioxidant activity. *J. Agric. Food Chem.* **2006**, *54*, 5806−5813.

(7) Sun, Z.; Fridrich, B.; de Santi, A.; Elangovan, S.; Barta, K. Bright side of lignin depolymerization: toward new platform chemicals. *Chem. Rev.* **2018**, *118*, 614−678.

(8) Mycroft, Z.; Gomis, M.; Mines, P.; Law, P.; Bugg, T. D. H. Biocatalytic conversion of lignin to aromatic dicarboxylic acids in Rhodococcus jostii RHA1 by re-routing aromatic degradation pathways. *Green Chem.* **2015**, *17*, 4974−4979.

(9) Akubo, K.; Nahil, M. A.; Williams, P. T. Pyrolysis-catalytic steam reforming of agricultural biomass wastes and biomass components for production of hydrogen/syngas. *J. Energy Inst.* **2019**, *92*, 1987−1996.

(10) Osada, M.; Sato, O.; Arai, K.; Shirai, M. Stability of supported ruthenium catalysts for lignin gasification in supercritical water. *Energy Fuels* **2006**, *20*, 2337−2343.

(11) Zhou, G.; Jensen, P. A.; Le, D. M.; Knudsen, N. O.; Jensen, A. D. Direct upgrading of fast pyrolysis lignin vapor over the HZSM-5 catalyst. *Green Chem.* **2016**, *18*, 1965−1975.

(12) Zhang, C.; Li, H.; Lu, J.; Zhang, X.; MacArthur, K. E.; Heggen, M.; Wang, F. Promoting lignin depolymerization and restraining the condensation via an oxidation−hydrogenation strategy. *ACS Catal.* **2017**, *7*, 3419−3429.

(13) Thring, R. W.; Breau, J. Hydrocracking of solvolysis lignin in a batch reactor. *Fuel* **1996**, *75*, 795−800.

(14) Barbier, J.; Charon, N.; Dupassieux, N.; Loppinet-Serani, A.; Mahé, L.; Ponthus, J.; Courtiade, M.; Ducrozet, A.; Quoineaud, A. A.; Cansell, F. Hydrothermal conversion of lignin compounds. A detailed study of fragmentation and condensation reaction pathways. *Biomass Bioenergy* **2012**, *46*, 479−491.

(15) Huang, X.; Korányi, T. I.; Boot, M. D.; Hensen, E. J. Catalytic depolymerization of lignin in supercritical ethanol. *ChemSusChem* **2014**, *7*, 2276−2288.

(16) Pandey, M. P.; Kim, C. S. Lignin depolymerization and conversion: a review of thermochemical methods. *Chem. Eng. Technol.* **2011**, *34*, 29−41.

(17) Chen, Q.; Marshall, M. N.; Geib, S. M.; Tien, M.; Richard, T. L. Effects of laccase on lignin depolymerization and enzymatic hydrolysis of ensiled corn stover. *Bioresour. Technol.* **2012**, *117*, 186−192.

(18) Zhang, J.; Chen, Y.; Brook, M. A. Effects of laccase on lignin depolymerization and enzymatic hydrolysis of ensiled corn stover. *ACS Sustainable Chem. Eng.* **2014**, *2*, 1983−1991.

(19) De Gregorio, G. F.; Prado, R.; Vriamont, C.; Erdocia, X.; Labidi, J.; Hallett, J. P.; Welton, T. Oxidative depolymerization of lignin using a novel polyoxometalate-protic ionic liquid system. *ACS Sustainable Chem. Eng.* **2016**, *4*, 6031−6036.

(20) Dabral, S.; Wotruba, H.; Herna′ndez, J. G.; Bolm, C. Mechanochemical oxidation and cleavage of lignin β-O-4 model compounds and lignin. *ACS Sustainable Chem. Eng.* **2018**, *6*, 3242−3254.

(21) Abdelaziz, O. Y.; Ravi, K.; Mittermeier, F.; Meier, S.; Riisager, A.; Lidén, G.; Hulteberg, C. P. Oxidative Depolymerization of Kraft Lignin for Microbial Conversion. *ACS Sustainable Chem. Eng.* **2019**, *7*, 11640−11652.

(22) Patankar, S. C.; Liu, L. Y.; Ji, L.; Ayakar, S.; Yadav, V.; Renneckar, S. Isolation of phenolic monomers from kraft lignin using a magnetically recyclable TEMPO nanocatalyst. *Green Chem.* **2019**, *21*, 785−791.

(23) Yang, W.; Du, X.; Liu, W.; Tricker, A. W.; Dai, H.; Deng, Y. Highly Efficient Lignin Depolymerization via Effective Inhibition of

Condensation during Polyoxometalate-Mediated Oxidation. *Energy Fuels* **2019**, *33*, 6483−6490.
(24) Fache, M.; Boutevin, B.; Caillol, S. Vanillin production from lignin and its use as a renewable chemical. *ACS Sustainable Chem. Eng.* **2016**, *4*, 35−46.
(25) Pinto, P. C. R.; Silva, E. A. B.; Rodrigues, A. E. Lignin as Source of Fine Chemicals: Vanillin and Syringaldehyde. In *Biomass Conversion*; Baskar, C.; Baskar, S.; Dhillon, R. S., Eds.; Springer: London, 2012; pp 381−420.
(26) Adachi, S.; Tanimoto, M.; Tanakal, M.; Matsuno, R. Kinetics of the alkaline nitrobenzene oxidation of lignin in rice straw. *Chem. Eng. J.* **1992**, *49*, B17−B21.
(27) Hasegawa, I.; Inoue, Y.; Muranaka, Y.; Yasukawa, T.; Mae, K. Selective production of organic acids and depolymerization of lignin by hydrothermal oxidation with diluted hydrogen peroxide. *Energy Fuels* **2011**, *25*, 791−796.
(28) Movil-Cabrera, O.; Rodriguez-Silva, A.; Arroyo-Torres, C.; Staser, J. A. Electrochemical conversion of lignin to useful chemicals. *Biomass Bioenergy* **2016**, *88*, 89−96.
(29) Deng, H.; Lin, L.; Sun, Y.; Pang, C.; Zhuang, J.; Ouyang, P.; Li, Z.; Liu, S. Perovskite-type oxide $LaMnO_3$: an efficient and recyclable heterogeneous catalyst for the wet aerobic oxidation of lignin to aromatic aldehydes. *Catal. Lett.* **2008**, *126*, 106−111.
(30) Bengoechea, M. O.; Hertzberg, A.; Miletić, N.; Arias, P. L.; Barth, T. Simultaneous catalytic de-polymerization and hydro-deoxygenation of lignin in water/formic acid media with Rh/Al_2O_3, Ru/Al_2O_3 and Pd/Al_2O_3 as bifunctional catalysts. *J. Anal. Appl. Pyrolysis* **2015**, *113*, 713−722.
(31) Zhang, J.; Deng, H.; Lin, L. Wet aerobic oxidation of lignin into aromatic aldehydes catalysed by a perovskite-type oxide: $La-Fe_{1-x}Cu_xO_3$ (x = 0, 0.1, 0.2). *Molecules* **2009**, *14*, No. 2747.
(32) Rahimi, A.; Azarpira, A.; Kim, H.; Ralph, J.; Stahl, S. S. Chemoselective metal-free aerobic alcohol oxidation in lignin. *J. Am. Chem. Soc.* **2013**, *135*, 6415−6418.
(33) Rahimi, A.; Ulbrich, A.; Coon, J. J.; Stahl, S. S. Formic-acid-induced depolymerization of oxidized lignin to aromatics. *Nature* **2014**, *515*, 249−252.
(34) Figueirêdo, M. B.; Heeres, H. J.; Deuss, P. J. Ozone mediated depolymerization and solvolysis of technical lignins under ambient conditions in ethanol. *Sustainable Energy Fuels* **2020**, *4*, 265−276.
(35) Aulin-Erdtman, G.; et al. Studies on the degradation of lignin and model compounds. I. The configuration of dehydrodiisoeugenol. *Acta Chem. Scand.* **1963**, *17*, 535−536.
(36) Tolba, R.; Tian, M.; Wen, J.; Jiang, Z. H.; Chen, A. Electrochemical oxidation of lignin at IrO_2-based oxide electrodes. *J. Electroanal. Chem.* **2010**, *649*, 9−15.
(37) Zhu, H.; Wang, L.; Chen, Y.; Li, G.; Li, H.; Tang, Y.; Wan, P. Electrochemical depolymerization of lignin into renewable aromatic compounds in a non-diaphragm electrolytic cell. *RSC Adv.* **2014**, *4*, 29917−29924.
(38) Wang, Y. S.; Yang, F.; Liu, Z. H.; Yuan, L.; Li, G. Electrocatalytic degradation of aspen lignin over Pb/PbO_2 electrode in alkali solution. *Catal. Commun.* **2015**, *67*, 49−53.
(39) Pan, K.; Tian, M.; Jiang, Z. H.; Kjartanson, B.; Chen, A. Electrochemical oxidation of lignin at lead dioxide nanoparticles photoelectrodeposited on TiO_2 nanotube arrays. *Electrochim. Acta* **2012**, *60*, 147−153.
(40) Rafiee, M.; Alherech, M.; Karlen, S. D.; Stahl, S. S. Electrochemical aminoxyl-mediated oxidation of primary alcohols in lignin to carboxylic acids: polymer modification and depolymerization. *J. Am. Chem. Soc.* **2019**, *141*, 15266−15276.
(41) Garedew, M.; Lin, F.; Song, B.; DeWinter, T. M.; Jackson, J. E.; Saffron, C. M.; Lam, C. H.; Anastas, P. T. Greener Routes to Biomass Waste Valorization: Lignin Transformation Through Electrocatalysis for Renewable Chemicals and Fuels Production. *ChemSusChem* **2020**, *13*, 1−25.
(42) Smith, C. Z.; Utley, J. H. P.; Hammond, J. K. Electro-organic reactions. Part 60[1]. The electro-oxidative conversion at laboratory scale of a lignosulfonate into vanillin in an FM01 filter press flow reactor: preparative and mechanistic aspects. *J. Appl. Electrochem.* **2011**, *41*, 363−375.
(43) Huang, Y.; Sun, S.; Huang, C.; Yong, Q.; Elder, T.; Tu, M. Stimulation and inhibition of enzymatic hydrolysis by organosolv lignins as determined by zeta potential and hydrophobicity. *Biotechnol. Biofuels* **2017**, *10*, No. 162.
(44) Singh, R. N.; Singh, A.; Mishra, D.; et al. Influence of the nature of conductive support on the electrocatalytic activity of electro-deposited Ni films towards methanol oxidation in 1 M KOH. *Int. J. Hydrogen Energy* **2008**, *33*, 6878−6885.
(45) Zirbes, M.; Quadri, L. L.; Breiner, M.; Stenglein, A.; Bomm, A.; Schade, W.; Waldvogel, S. R. High-temperature electrolysis of Kraft lignin for selective vanillin formation. *ACS Sustainable Chem. Eng.* **2020**, *8*, 7300−7307.
(46) Schmitt, D.; Regenbrecht, C.; Hartmer, M.; Stecker, F.; Waldvogel, S. R. Highly selective generation of vanillin by anodic degradation of lignin: a combined approach of electrochemistry and product isolation by adsorption. *Beilstein J. Org. Chem.* **2015**, *11*, 473−480.
(47) Klinke, H. B.; Thomsen, A. B.; Ahring, B. K. Inhibition of ethanol-producing yeast and bacteria by degradation products produced during pre-treatment of biomass. *Appl. Microbiol. Biotechnol.* **2004**, *66*, 10−26.
(48) Heikkinen, S.; Toikka, M. M.; Karhunen, P. T.; Kilpeläinen, I. A. Quantitative 2D HSQC (Q-HSQC) via Suppression of J-Dependence of Polarization Transfer in NMR Spectroscopy: Application to Wood Lignin. *J. Am. Chem. Soc.* **2003**, *125*, 4362−4367.
(49) You, B.; Liu, X.; Liu, X.; Sun, Y. Efficient H_2 evolution coupled with oxidative refining of alcohols via a hierarchically porous nickel bifunctional electrocatalyst. *ACS Catal.* **2017**, *7*, 4564−4570.

https://dx.doi.org/10.1021/acs.energyfuels.0c02284
Energy Fuels 2020, 34, 12703−12709